IMAGE RECTIFICATION USING A GENERIC SENSOR MODEL – RATIONAL FUNCTION MODEL

C. Vincent TAO, Yong HU
Department of Geomatics Engineering, The University of Calgary, Canada
ctao@ucalgary.ca, yhu@ucalgary.ca

J. Bryan MERCER, Steve SCHNICK
Intermap Technologies Ltd., Canada
bmercer@intermap.ca,

Yun ZHANG
Department of Geodesy and Geomatics Engineering, University of New Brunswick, Canada
yunzhang@unb.ca

WG IV/4

KEY WORDS: Sensor Model, SAR, Polynomial Model, Rational Function Model, Rectification.

ABSTRACT

The Rational Function Model (RFM) has been considered as a generic sensor model. Compared to polynomial models widely used, RFM is essentially a more generic and expressive form. The RFM is technically applicable to all types of sensors such as frame, pushbroom, whiskbroom and SAR etc. With the increasing availability of the new generation imaging sensors, accurate and fast rectification of digital imagery using a generic sensor model becomes of great interest to the user community. In this paper, the technical viability of use of the RFM is examined. This paper firstly presents a brief overview of the geometric models used for the rectification of digital imagery. These models are the collinear equations based differential rectification model, the polynomial model, the projective transform model, the extended direct linear transform model and the RFM. The remarks on their properties, and the advantages and disadvantages for different models are discussed so that one will have a better understanding of the generic nature of the RFM. The two solution methods to the RFM, namely direct solution and iterative solution, are then provided. In fact, iterative solution is more rigorous in theory but requires many iterative steps to achieve the solution. Finally, the test results using real-world data sets are described. Comprehensive experiments have been carried out to evaluate the viability of the RFM solutions.

1 BACKGROUND

Sensor models are required to restitute the functional relationships between the image plane and the ground space. They can be grouped into two classes, physical sensor models and generalized sensor models. Physical sensor models are more rigorous and normally provide better accuracies since the model parameters employed represent the physical imaging process of sensors. However, building of a physical sensor model requires information of the physical sensor and its imaging model. It is realized that this information is not always available, especially for images from commercial satellites (e.g., IKONOS). The generalized sensor models are independent on sensor platforms as well as sensor types. Such properties have made generalized sensor models very popular in the remote sensing community. The typical generalized sensor models are polynomial-based ones. Their capabilities have been widely tested and examined.

The RFM is essentially a generic form of polynomial models. However, there are few publications that address its viability, accuracy and stability. In Tao and Hu (2000), the numerical properties of the RFM and its detailed least square solutions are investigated and documented. The RFM solution has been tested using various data sets including simulated data, aerial photogrammetry data as well as SPOT data. In this paper, we describe results of the recent tests conduced in conjunction with the Intermap Technologies Corporation, Canada.

The objective of this work is to test the viability of the use of RFM to image rectification using Intermap SAR (synthetic aperture radar) imagery and DEMs obtained from Intermap STAR-3i system. STAR-3i is an X-band, interferometric airborne SAR system that is owned and commercially operated by Intermap Technologies. The system is able to produce DEMs with sample spacing of 2.5 meter and with vertical accuracy at the meter to sub-meter level (Bryan and Schnick, 1999). The system can also produce ortho-rectified SAR magnitude imagery (ORIs) by using direct GPS/INS georeferencing technology. In fact, both DEMs and ORIs are created simultaneously as part of STAR-3i processing. With the utilization of the ORIs and DEMs, the image rectification process can be simplified since the

ORIs can be used as a ground reference "map" and the "ground" control points can be selected directly from the ORIs. It can be seen that an accurate and generalized sensor model is of particular importance to leverage the commercial applicability and enlarge the market for Intermap's products, DEMs and ORIs. We, therefore, investigated RFM under this context.

2 GEOMETRIC MODELS FOR IMAGE RECTIFICATION

2.1 Collinear Equations based Differential Rectification

Collinear equations are rigorous models available for frame and pushbroom sensors. For frame images, it is described as

$$x = x_p - c\frac{r_{11}(X - X_0) + r_{21}(Y - Y_0) + r_{31}(Z - Z_0)}{r_{13}(X - X_0) + r_{23}(Y - Y_0) + r_{33}(Z - Z_0)} = f_x(x', y') \tag{1}$$

$$y = y_p - c\frac{r_{12}(X - X_0) + r_{22}(Y - Y_0) + r_{32}(Z - Z_0)}{r_{13}(X - X_0) + r_{23}(Y - Y_0) + r_{33}(Z - Z_0)} = f_y(x', y')$$

Where *X, Y, Z* are three-dimensional coordinates defined by a DEM pixel; *x, y* are the corresponded position in the image which are transformed by the collinear equation; and *x'*, *y'* are equivalent to the map (DEM) coordinates *X*, *Y*.

For line scanning sensors (e.g. SPOT), the mathematical model has to be modified to line-perspective geometry:

$$x = -c\frac{r^i_{11}(X - X_{i0}) + r^i_{21}(Y - Y_{i0}) + r^i_{31}(Z - Z_{i0})}{r^i_{13}(X - X_{i0}) + r^i_{23}(Y - Y_{i0}) + r^i_{33}(Z - Z_{i0})} = f_x(x', y') \tag{2}$$

$$0 = -c\frac{r^i_{12}(X - X_{i0}) + r^i_{22}(Y - Y_{i0}) + r^i_{32}(Z - Z_{i0})}{r^i_{13}(X - X_{i0}) + r^i_{23}(Y - Y_{i0}) + r^i_{33}(Z - Z_{i0})} = f_y(x', y')$$

Where x_i is the coordinate in scan-line i, orthogonal to the direction of travel, and x_p, $y_p = 0$.

Remarks:

- Image domain corrections can be utilized for removing camera distortions
- Triangulation is possible so that both systematic and random errors can be reduced to a great deal.
- This is a rigorous model with both relief displacements and camera distortions corrected.
- Specified information about interior orientation, exterior orientation of the sensor and other related orbital data are required.
- Software must be changed for each different image sensor.
- It is mathematically complex with long execution time.
- The imaging parameters are not always available, e.g., IKONOS, for the use of this model.

2.2 Polynomial Rectification: 2D and 3D

When the image area is flat, polynomials with a low order can serve accurate results. In this case the model can be represented as a 2D model:

$$x = a_0 + a_1X + a_2Y \tag{3}$$
$$y = b_0 + b_1X + b_2Y$$

Where *x, y* are the pixel position in the image; *X, Y* are the coordinates on ground (map); and a_0, a_1, a_2, b_0, b_1, b_2 are polynomial coefficients.

Some studies have shown that the use of low-order polynomial 3D models for rectifying images in hilly and mountainous areas can reach the accuracy level that is close to the rigorous models (Palà and Pons 1995, Okamoto et al. 1999). For example, a typical formula is:

$$x = a_0 + a_1X + a_2Y + a_3Z + a_4XZ + a_5YZ \tag{4}$$
$$y = b_0 + b_1X + b_2Y + b_3Z + b_4XZ + b_5YZ$$

Where *X, Y, Z* are the ground coordinates and height respectively.

Remarks:
- The model is simple and computationally fast.
- It is independent of the sensor geometry and platform.
- Applicable when the relief displacement does not influence the result significantly.
- Polynomial expressions are characterized by a great capability for absorption of accidental distortions.
- Accuracy is less than rigorous models in general.
- For the inexperienced user a high-order polynomial may seem to provide a perfect fit at the reference points, as the residuals are small. However, undulations between the reference points occurred could create large errors.

2.3 Projective Transformation

The projective transform describes the relationship between two planes. It is defined by eight parameters, which can be derived from four object points lying in a plane and their corresponding image coordinates.

$$x = \frac{a_1 x' + a_2 y' + a_3}{c_1 x' + c_2 y' + 1} = f_x(x', y') \tag{5}$$

$$y = \frac{b_1 x' + b_2 y' + b_3}{c_1 x' + c_2 y' + 1} = f_y(x', y')$$

Where *x, y* are coordinates of the original image; *x', y'* are coordinates of the rectification; and a_1, a_2, a_3, b_1, b_2, b_3, c_1, c_2 are projective parameters.

For the images of pushbroom sensors the projective transformation can be modified as:

$$x = \frac{a_1 x' + a_2 y' + a_3}{c_1 x' + c_2 y' + 1} = f_x(x', y') \tag{6}$$

$$y = b_1 x' + b_2 y' + b_3 = f_y(x', y')$$

where *y* is given in the flying direction and *x* represents the pixel in a scan line. Compared to (1), the elements of exterior and interior orientations are implicit in these parameters

Remarks:
- This method is typically used to rectify aerial photographs of flat terrain or image of facades of buildings (Novak, 1992).
- The elements of exterior and interior orientation are not required, as they are implicit in the eight parameters.
- This method has little practical significance for satellite sensors, but could be applied for airborne line scanners.

2.4 Extended Direct Linear Transformation (DLT) Model: 3D

The mode was investigated by Okamoto, et al. (1999) and has been compared with other models for SPOT rectification.

$$x_c = \frac{a_1 X + a_2 Y + a_3 Z + a_4}{a_9 X + a_{10} Y + a_{11} Z + 1} + a_{12} x_c y_c \tag{7}$$

$$y_c = \frac{a_5 X + a_6 Y + a_7 Z + a_8}{a_9 X + a_{10} Y + a_{11} Z + 1} + a_{13} y_c^2$$

Where x_c, y_c are the coordinates on the image, and *X, Y, Z* are the coordinates on the ground.

Remarks:
- With the extended DLT model, the acquisition of approximate values is quite straightforward.
- Individual orientation parameters are not required in many instances.

- The presence of the additional parameters helps to account for wider field angles of the scanner, and the additional parameter a_{12} has proven most effective for SPOT imagery.
- With this model, although a reasonable degree of geometric stability is obtained, triangulation results can be expected to deteriorate when only a small number of GCPs are available.

3 A GENERIC SENSOR MODEL - RATIONAL FUNCTION MODEL

The RFM uses a ratio of two polynomial functions to compute the x coordinate in the image, and a similar ratio to compute the y coordinate in the image.

$$x = \frac{p1(X,Y,Z)}{p2(X,Y,Z)} = \frac{\sum_{i=0}^{m1}\sum_{j=0}^{m2}\sum_{k=0}^{m3} a_{ijk} X^i Y^j Z^k}{\sum_{i=0}^{n1}\sum_{j=0}^{n2}\sum_{k=0}^{n3} b_{ijk} X^i Y^j Z^k} \tag{8}$$

$$y = \frac{p3(X,Y,Z)}{p4(X,Y,Z)} = \frac{\sum_{i=0}^{m1}\sum_{j=0}^{m2}\sum_{k=0}^{m3} c_{ijk} X^i Y^j Z^k}{\sum_{i=0}^{n1}\sum_{j=0}^{n2}\sum_{k=0}^{n3} d_{ijk} X^i Y^j Z^k}$$

Where x, y are normalized pixel coordinates on the image; X, Y, Z are normalized 3D coordinates on the ground (map and DEM), and a_{ijk}, b_{ijk}, c_{ijk}, d_{ijk} are polynomial coefficients.

The above equations can be rewritten as follows:

$$r = \frac{\begin{pmatrix}1 & Z & Y & X & \cdots & Y^3 & X^3\end{pmatrix}\cdot\begin{pmatrix}a_0 & a_1 & \cdots & a_{19}\end{pmatrix}^T}{\begin{pmatrix}1 & Z & Y & X & \cdots & Y^3 & X^3\end{pmatrix}\cdot\begin{pmatrix}1 & b_1 \cdots b_{19}\end{pmatrix}^T} \tag{9a}$$

$$c = \frac{\begin{pmatrix}1 & Z & Y & X & \cdots & Y^3 & X^3\end{pmatrix}\cdot\begin{pmatrix}c_0 & c_1 & \cdots & c_{19}\end{pmatrix}^T}{\begin{pmatrix}1 & Z & Y & X & \cdots & Y^3 & X^3\end{pmatrix}\cdot\begin{pmatrix}1 & d_1 \cdots d_{19}\end{pmatrix}^T} \tag{9b}$$

The polynomial coefficients are called rational function coefficients (RFCs). In general, distortions caused by optical projection can be represented by ratios of first-order terms, while corrections such as earth curvature, atmospheric refraction, and lens distortion etc., can be well approximated by second-order terms. Some other unknown distortions with high order components can be modeled using a RFM with third-order terms.

Direct vs. Iterative Lease Square Solution

Given a DEM and an image acquired from the same earth surface using some physical sensor, we assume that many object-image coordinate pairs of ground points (GPs) and corresponding image points (IPs) can be collected evenly over the entire ground area. Now, what we should do is to solve RFCs under rational function model using these GP/IP coordinate pairs, some of which are used as control coordinate pairs (CCPs) to solve RFCs, others are used as check ones (CKPs).

To solve the RFCs by a linear least squares method, first of all, equations (8) have to be linearized with respect to the RFCs. From equations (9), error equations can be written as:

$$v_r = \begin{bmatrix}\frac{1}{B} & \frac{Z}{B} & \frac{Y}{B} & \frac{X}{B} & \cdots & \frac{Y^3}{B} & \frac{X^3}{B} & -\frac{rZ}{B} & -\frac{rY}{B} & \cdots & -\frac{rY^3}{B} & -\frac{rX^3}{B}\end{bmatrix}\cdot J - \frac{r}{B} \tag{10a}$$

$$v_c = \begin{bmatrix}\frac{1}{D} & \frac{Z}{D} & \frac{Y}{D} & \frac{X}{D} & \cdots & \frac{Y^3}{D} & \frac{X^3}{D} & -\frac{cZ}{D} & -\frac{cY}{D} & \cdots & -\frac{cY^3}{D} & -\frac{cX^3}{D}\end{bmatrix}\cdot K - \frac{c}{D} \tag{10b}$$

or

$$Bv_r = [1 \quad Z \quad Y \quad X \quad \cdots \quad Y^3 \quad X^3 \quad -rZ \quad -rY \quad \cdots \quad -rY^3 \quad -rX^3]\cdot J - r \tag{11a}$$

$$Dv_c = [1 \quad Z \quad Y \quad X \quad \cdots \quad Y^3 \quad X^3 \quad -cZ \quad -cY \quad \cdots \quad -cY^3 \quad -cX^3] \cdot K - c \tag{11b}$$

Where

$$B = (1 \quad Z \quad Y \quad X \quad \cdots \quad Y^3 \quad X^3) \cdot (1 \quad b_1 \cdots b_{19})^T$$
$$J = (a_0 \quad a_1 \quad \cdots \quad a_{19} \quad b_1 \quad b_2 \quad \cdots \quad b_{19})^T$$
$$D = (1 \quad Z \quad Y \quad X \quad \cdots \quad Y^3 \quad X^3) \cdot (1 \quad d_1 \cdots d_{19})^T$$
$$K = (c_0 \quad c_1 \quad \cdots \quad c_{19} \quad d_1 \quad d_2 \quad \cdots \quad d_{19})^T$$

Given n CCPs, the following error equations can be used

$$\begin{bmatrix} V_r \\ -- \\ V_c \end{bmatrix} = \begin{bmatrix} M & | & 0 \\ -- & + & -- \\ 0 & | & N \end{bmatrix} \cdot \begin{bmatrix} J \\ -- \\ K \end{bmatrix} - \begin{bmatrix} R \\ -- \\ C \end{bmatrix}$$

$$V = T\,I - G$$

and the normal equation is

$$T^T W^2 T I - T^T W^2 G = 0 \tag{12}$$

Where,

$$M = \begin{bmatrix} 1 & Z_1 & \cdots & X_1^3 & -r_1 Z_1 & \cdots & -r_1 X_1^3 \\ 1 & Z_2 & \cdots & X_2^3 & -r_2 Z_2 & \cdots & -r_2 X_2^3 \\ \vdots & \vdots & \ddots & \vdots & \vdots & \ddots & \vdots \\ 1 & Z_n & \cdots & X_n^3 & -r_n Z_n & \cdots & -r_n X_n^3 \end{bmatrix}, \quad N = \begin{bmatrix} 1 & Z_1 & \cdots & X_1^3 & -c_1 Z_1 & \cdots & -c_1 X_1^3 \\ 1 & Z_2 & \cdots & X_2^3 & -c_2 Z_2 & \cdots & -c_2 X_2^3 \\ \vdots & \vdots & \ddots & \vdots & \vdots & \ddots & \vdots \\ 1 & Z_n & \cdots & X_n^3 & -c_n Z_n & \cdots & -c_n X_n^3 \end{bmatrix}, \quad R = \begin{bmatrix} r_1 \\ r_2 \\ \vdots \\ r_n \end{bmatrix}, \quad C = \begin{bmatrix} c_1 \\ c_2 \\ \vdots \\ c_n \end{bmatrix}$$

and W is the weight matrix:

$$W = \begin{bmatrix} W_r & 0 \\ 0 & W_c \end{bmatrix}, \quad W_r = \begin{bmatrix} \frac{1}{B_1} & 0 & \cdots & 0 \\ 0 & \frac{1}{B_2} & 0 & \vdots \\ \vdots & 0 & \ddots & 0 \\ 0 & \cdots & 0 & \frac{1}{B_n} \end{bmatrix}, \quad W_c = \begin{bmatrix} \frac{1}{D_1} & 0 & \cdots & 0 \\ 0 & \frac{1}{D_2} & 0 & \vdots \\ \vdots & 0 & \ddots & 0 \\ 0 & \cdots & 0 & \frac{1}{D_n} \end{bmatrix}$$

The direct solution to RFCs is given by setting W_r to be the identity matrix. In this case, equation (12) can be solved using a standard least square method.

As for the iterative solution, The initial value $I^{(0)}$ of the coefficients can be firstly solved using the direct solution method, then $W^{(i)}$ and $I^{(i)}$ will be calculated by solving the normal equation (12) iteratively until some termination condition is satisfied. For more details on the derivation of the equations, one can refer to Tao and Hu (2000).

Remarks:

- It is essentially a ***generic*** form of the models described in section 2. In fact, the collinearity model, the projective transform model, and the extended direct linear transform model are in the form of the RFM with the first order, while, the polynomial model is a special case of the RFM, when its denominator is equal to 1.
- In the polynomial functions, the three ground coordinates and the two image coordinates are each offset and scaled to have a range of from –1.0 to +1.0 over an image segment.
- The maximum power of each ground coordinate (m1, m2, m3, n1, n2, and n3) is limited to 3. Furthermore, the power of all the three ground coordinates is limited to 3. That is, the polynomial coefficients are defined to be zero whenever $i+j+k > 3$.

- One ratio of polynomial model can be used for all types of images.
- The same ratio model can be used by all exploitation software, producing the same errors and error estimates. This commonality will make enterprise wide error analysis easier.
- Exploitation software using the ratio model can be completely ignorant of the rigorous image geometry model used to create it. The rigorous image geometry model is thus easier to update as sensors evolve, since changes to it do not cascade into the exploitation software.
- Usually fit to a rigorous image geometry model with limited accuracy (not triangulated with several overlapping images).
- Complex fitting process, to avoid a denominator polynomial function going to zero within the image segment extent (producing excessive errors).

4 TEST RESULTS AND EVALUATION

4.1 Test Data Set

The test data set is provided by Intermap Technologies. A total of 50 control coordinate pairs well distributed in the image were manually collected from an ortho-rectified aerial image with 2.5 meters resolution (shown in Figure 1). Figure 2 provide a 3-D view of the distribution of these selected control points (marked by "•" dots). In Figure 2, the terrain was generated using a cubic interpolation based on a Delaunay triangulation of these points. An independent set of 49 points was collected as checkpoints from an ortho-rectified aerial image with 1 meter resolution, marked as "+" in Figure 2.

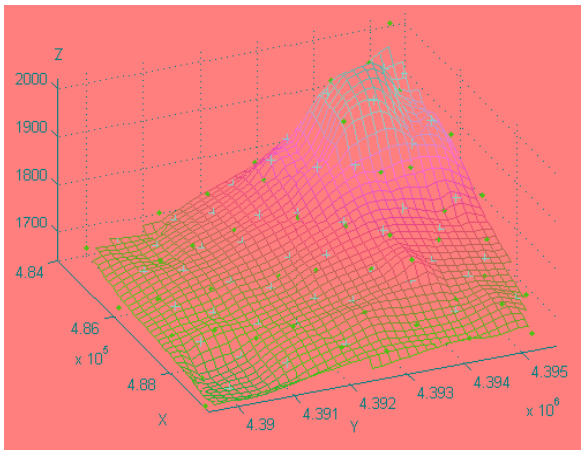

Figure 2 The distribution of control/check points in 3-D

Degree of RFM	Case	Number of RFCs	Min. number of CCPs required
6	$p2 \neq p4$	78	39
	$p2 = p4$	59	30
	$p2 = p4 \equiv 1$	40	20
4	$p2 \neq p4$	38	19
	$p2 = p4$	29	15
	$p2 = p4 \equiv 1$	20	10

Table 1 Test configuration of the RFM

Solution	four-degree				six-degree			
	at CCPs		at CKPs		at CCPs		at CKPs	
$p2 \neq p4$	rms	max	rms	max	rms	max	rms	max
Direct	1.06e+00	2.62e+00	1.15e+00	3.45e+00	8.42e-01	2.05e+00	1.40e+00	3.68e+00
Iterative	9.32e-01	2.34e+00	1.02e+00	2.80e+00	8.39e-01	2.09e+00	1.42e+00	3.81e+00
PCI	1.05e+00	2.50e+00	1.19e+00	3.59e+00	8.77e-01	2.40e+00	1.28e+00	3.01e+00
$p2 = p4$	rms	max	rms	max	rms	max	rms	max
Direct	1.24e+00	2.73e+00	1.11e+00	3.27e+00	9.05e-01	2.26e+00	1.28e+00	3.14e+00
Iterative	1.05e+00	2.14e+00	1.03e+00	2.50e+00	9.03e-01	2.29e+00	1.29e+00	3.11e+00
$p2 = p4 \equiv 1$	rms	max	rms	max	rms	max	rms	max
Direct	1.17e+00	2.50e+00	1.10e+00	3.06e+00	9.78e-01	2.23e+00	1.24e+00	3.90e+00

Table 2 Residuals in image with the test data set (unit: pixel)

4.2 Results and Evaluation

In order to compare the solution methods to RFM, both direct and iterative solutions were tested. We have also tested the RFM performance under the different parameter configurations. As shown in Table 1, third-order RFM (i.e., degree is 6) and second-order RFM (i.e., degree is 4) are tested under the following cases: (a) p2≠ p4 with 78 or 38 unknown RFCs; (b) p2=p4 with 59 or 29 unknowns; and (c) p2=p4=1, regular polynomials with 40 or 20 unknowns.

PCI software supports several sensor models including the rational function model. The results computed using the PCI RFM module are also given in Table 2. Both the root mean square (RMS) of the residuals and the maximum errors at control points and checkpoints in image are listed. Based on the analysis of these results, the following observations are obtained:

- Both the rational function models and the polynomial model (i.e., p2=p4=1 case) can reach the accuracy around 1 pixel.
- In general, the cases with rational components are slightly better than the polynomial models.
- The fitting accuracy of the cases with four-degree is very close to those with six-degree. It is understandable since the aerial photogrammetry data set may not involve high order distortions.
- The accuracy of the direct solution method is comparable with that of the iterative solution method when the number of control points (i.e., 50 or more) are enough. The iterative solution is often slightly better than the direct solution when only a few more control points than the minimum number of control points required are available.

5 CONCLUSIONS

An overview of sensor models are given in this paper. These models are the collinearity equations based differential rectification model, the polynomial model, the projective transform model, the extended direct linear transform model and the rational function model. The remarks on their properties, and advantages and disadvantages are also discussed. It can be observed that the RFM is essentially a generic form of the all described models.

Unlike the physical sensor models, the rational function model needs no knowledge specific to each type of imaging sensor physics, such as orbit parameters and platform orientation parameters. It has been noticed that rigorous models are not always available, especially for images from commercial stateliness (e.g., IKONOS), where the rigorous sensor model is hidden to the end user. Therefore, the RFM becomes an alternative sensor model to image rectification.

For aerial optical images (i.e., frame sensor type), the test results show that both the rational function model and the polynomial model can reach reasonably good accuracy. Because the fitting accuracy of the cases with four-degree RFM is almost the same with those with six-degree RFM, high order forms are often not necessary. The iterative solution method to RFM provides a better accuracy than the direct solution method, but the direct solution method is usually adequate when enough control points are available.

REFERNENCES

Chen, L.C., Lee, L.H., 1993. Rigorous generation of digital orthophotos from SPOT images. Photogrammetric Engineering and Remote Sensing 59(5): 655-61.

Greve, C. W., 1992. Image processing on open systems, Photogrammetric Engineering and Remote Sensing, 58(1): 85-89.

Mercer, B., Schnick, S, 1999.Comparison of DEMs from SATR-3i Interferometric SAR and Scanning Laser, ISPRS Commission III, Workshop, La Jolla, CA, November 9-11, 1999.

Novak, K., 1992. Rectification of digital imagery. Photogrammetric Engineering and Remote Sensing, 58(3), pp. 339-344.

OpenGIS Consortium, 1999. The OpenGIS Abstract Specification - Topic 7: The Earth Imagery Case, http://www.opengis.org/public/abstract/99-107.pdf.

Okamoto, A., Ono, T., Akamatsu, S., Fraser, C., Hattori, S., Hasegawa, H., 1999. Geometric characteristics of alternative triangulation models for satellite imagery. Proceedings of 1999 ASPRS Annual Conference, From Image to Information, Oregon, May 17-21.

Palà, V., Pans, X., 1995. Incorporation of relief in polynomial-based geometric corrections. PE&RS, 61(7), pp. 935-44.

Tao, C.V. and Hu, Y., 2000. Investigation of the Rational Function Model, Proceedings of ASPRS Annual Conversion, Washington D.C, May 22-26, 2000

Toutin, T., 1995. Multisource data fusion with an integrated and unified geometric modeling. EARSeL Advances in Remote Sensing, Vol. 4, No. 2, pp. 118-129.

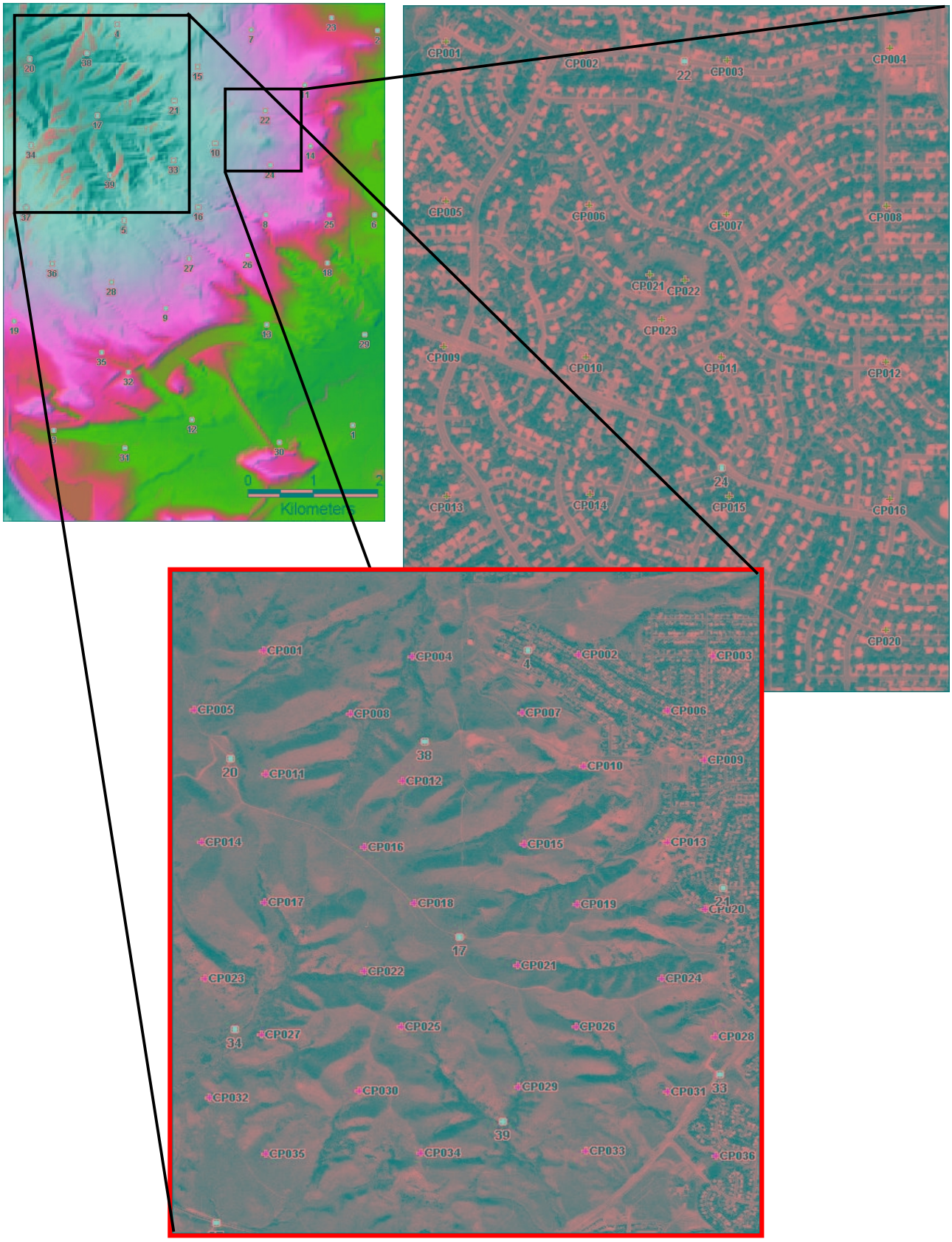

Figure 1. Test DEMs (left top) and images (up image-flat residential area, bottom image-ridge areas). Red dots are selected control points and green dots are chosen checkpoints.